# FLUCTUATING STATIC PRESSURE MEASUREMENTS IN THE ALLIED AEROSPACE NORTH AMERICAN 7 X 7 FOOT TRISONIC WIND TUNNEL

**BORIS L. MEDVED*, CHARLES A. RADOVICH****

**Allied Aerospace Industries**
**400 Duley Road, El Segundo, CA 90245, USA**
***310 335-1585/718 Fax 310 640-1056 bmedved@alliedaerospace.com**
****310 335-1585/718 Fax 310 640-1056 cradovich@alliedaerospace.com**

**Keywords**: *wind tunnel, static pressure fluctuations, perforated walls, acoustics, edge-tones*

## Abstract

*In order to understand the physical nature of noise source generation mechanisms and their propagation paths in the Allied Aerospace North American 7 x 7 foot Trisonic Wind Tunnel (TWT) static pressure fluctuations have been investigated in both porous and solid test sections. Measurements were performed in the Mach number range of 0.6 to 3.0, and frequency range of 0 Hz to 40 kHz. A ten-degree cone probe, specifically designed for the investigation, along with a number of high-frequency transducers located on the wind tunnel walls, were used to collect high-frequency data. While the overall noise level in the TWT porous test section at transonic speeds is comparable to other major industrial transonic facilities, the existence of discrete frequencies as significant contributors to the overall sound energy level deserves attention. It was found that most energy contents are located below 1 kHz (i.e., both broadband noise and discrete frequencies). However, most dominant resonant spikes are evident at frequencies greater than 9 kHz due to edge-tones generated by the perforated walls. Edge-tone noise is produced by an interaction between the shear layer and the trailing edge of the perforations.*

## 1 Introduction

### 1.1 Wind Tunnel Description

The following section offers a brief description of the principal features of the tunnel. The Allied Aerospace Trisonic Wind Tunnel, located approximately one mile south of Los Angeles International Airport (LAX), is an intermittent blowdown facility with a 7 x 7 foot tandem test section capable of testing aerodynamic, propulsion and aeroelastic models over a range from Mach 0.1 to 3.5. The facility, shown in Figure 1, is available for use by other companies.

Centrifugal compressors supply air at 40-lbs/sec to eight spherical storage tanks with a combined total volume of 214,000-ft$^3$. The air is dried to a dew point of roughly -35° F (-37° C) and stored at a pressure of 10 atmospheres.

Flow from the storage spheres is regulated by an 8-ft diameter servo-controlled valve which holds a pre-selected pressure in the settling chamber. Downstream of the settling chamber, the air passes through a fixed transition and a variable nozzle. The floor and ceiling of the nozzle may be contoured to produce supersonic velocities in the test section.

Subsonic and transonic Mach numbers are controlled by setting a variable diffuser

downstream of the test section. A pair of servo-controlled flaps on the centerline strut in the variable diffuser operates to compensate for changes in blockage caused by pitching a model during a blow. During the blow, these flaps maintain a constant Mach number within ±0.005 or less.

Two 7 x 7 foot test sections, one with solid walls for supersonic testing and the other with porous walls for transonic and subsonic testing are permanently installed in a tandem arrangement as shown in Figure 2. The porous walls have normal holes, 0.25-in in diameter, resulting in a fixed porosity level of 19.7%. Supersonic testing may also be done in the porous wall test section, but with a slightly less uniform Mach number distribution when compared to the solid wall test section. An access door with a maximum opening of 6-ft wide by 7-ft high exists in the variable diffuser.

Downstream of the variable diffuser, the air is decelerated in a fixed diffuser with a 5-degree equivalent expansion angle. The diffuser terminates in a sound abatement muffler building where the air is exhausted vertically to the atmosphere.

## 2 Static Pressure Fluctuation Investigation

### 2.1 Static Pressure Fluctuations

Static pressure fluctuations were measured in both porous and solid test sections. A newly designed ten-degree cone probe with two flush-mounted high-frequency transducers was used to measure static pressure fluctuations at the test sections centerline. In addition, five high-frequency transducers were installed on the wind tunnel walls (one on the solid test section wall, two on the perforated test section wall and two on the high-speed diffuser floor). Their installation was part of an effort to understand the principal sources of noise generation and the acoustic propagation paths along the wind tunnel circuit [1, 2, 3].

### 2.2 Cone Probe

Fluctuating static pressures were measured in both porous and solid wall test sections using the ten-degree cone probe. The probe, shown in Figure 3, was 24.77-in. in length and 2.76-in. in diameter, resulting in less than 0.1% blockage. A picture of the cone probe installed in the solid test section is shown in Figure 4. General locations of the cone probe tip in the solid and porous wall test sections are also given in Figure 2.

### 2.3 Cone Probe Transducers

Two Kulite differential transducers, model XCQ-080-25D, were installed on the cone probe 6.0-in aft of the cone tip, 180-degrees apart. The chosen location of the high-frequency transducers represented a compromise between two conflicting considerations:

1) Forward position puts the transducer in the (quieter) laminar boundary layer
2) Aft position (greater cone diameter) gives fewer disturbances from the edge of the installation holes

### 2.4 Wall Mounted Transducers

Five Kulite absolute transducers, model LQ-5-080-25A, were used to take measurements on the walls. Their locations are shown in Figure 2. In the figure, the transducers are labeled STS (solid test section), TS1 and TS2 (porous test section), and DIFF1 and DIFF2 (diffuser floor). The STS and TS1 Kulites were flush-mounted on the west wall at the same test section locations as the cone probe. TS2 was located 3.0-in downstream of TS1. These adjacent sensors were to assist in determining the direction acoustics disturbances propagate. DIFF1 and DIFF2 were installed on opposite sides of the diffuser floor.

### 2.5 Transducer Calibration

Prior to installation, all high-frequency transducers were calibrated for a steady-state pressure response. After installation, a dynamic calibration was performed (one point, end-to-

end) using a B&K Pistonphone, Model 4228, at a frequency of 250 Hz and a SPL of 124 dB.

### 2.6 Data Acquisition and Spectral Analysis

A Yokogawa ScopeCorder, Model DL-750, high-speed data acquisition system was used to collect data. All high-frequency channels were sampled at 200 kHz and were coupled with a 40 kHz low pass, two-pole Bessel, analog filter.

### 2.7 Statistical Reliability of Spectral Data

The major factors effecting statistical analysis of random data are finite sample length, random error and systematic error [4, 5]. Bendatt and Piersol also indicate that the normalized random error for a power spectral density estimate is inversely proportional to the square root of the number of averages used in computation. For this investigation, one hundred averages were used. This scenario resulted in a normalized random error of ten percent for the power spectral density data. Spectral analysis for the centerline and wall transducers was performed by means of Welch's method using a Hanning window with 50% overlap.

### 2.8 Reynolds Number Considerations

All the blows were performed at the facility minimum Reynolds numbers since it had been learned from many similar investigations that fluctuating static pressure is not a strong function of Reynolds number.

## 3 Results and Discussions

### 3.1 Porous Test Section

As shown in Figure 5, the two Kulite high-frequency differential transducers installed on the ten-degree cone probe (Cone 1 and Cone 2) indicated very similar outputs. Therefore, only the results from the transducer at zero degrees roll (Cone 1) will be shown.

An overall noise level comparison with a number of major industrial continuous and two blowdown transonic wind tunnels is shown in Figure 6. As seen from the figure, the TWT static pressure fluctuations level at the centerline (Cone 1) is comparable to most industrial transonic wind tunnels. However, when comparing noise levels, the differences in the instrumentation used in different wind tunnels should be noted. This is especially true for differences in measured frequency ranges, which can ultimately generate very different pictures for overall noise levels.

Representative power spectral density plots at Mach numbers 0.6, 0.8, 1.1 and 1.2 are shown in Figures 7 through 15 for the centerline cone probe and the diffuser floor transducers. When dealing with static pressure fluctuations in wind tunnels, especially transonic ones, it is difficult to pinpoint acoustics generation sources, their related generation mechanisms and their paths along the wind tunnel circuit. Therefore, a logical choice is to focus on those phenomena that are believed to be explainable and leave those uncertain ones for discussion and further analysis.

At the centerline, at M = 0.6, a resonant peak exists at approximately 16 Hz (Figure 7). This peak corresponds to the length of the lower plenum chamber (31-ft) indicating a close-close longitudinal resonance mode. Using the responses from the two adjacent transducers located on the perforated test section wall (TS1 and TS2) the direction of propagation was determined for this resonance mode. As shown in Figure 8, at 16 Hz the phase is positive, indicating upstream propagation. Therefore, at subsonic speeds, this type of acoustic disturbance propagates through the sector slot (located at the downstream edge of the porous test section) through test section/diffuser step, and through the perforated walls into the porous test section.

Also in Figure 7, three broadband "humps" can be seen at higher frequencies of approximately 200 Hz, 3 kHz and 9 kHz. The 200 Hz hump has many spikes that might be related to either the complex plenum chamber structure or the

control valve. The origin of the 3 kHz hump is undetermined, but it should be noted that the amplitude in the porous test section decreases with increasing Mach number and is undetectable in the solid test section. The 9 kHz hump is related to edge-tones generated by a shear layer interaction with the ¼-in normal perforations on the test section walls. Edge-tones are Mach number dependent disturbances that develop due to flow across a cavity or open perforation. Given a characteristic length, L, the frequencies generated by the perforations can be predicted for a range of Mach numbers, M, using Equation 1,

$$f = \frac{U(m-a)}{L\left(\frac{1}{k} + \frac{M}{\sqrt{1+0.5(g-1)M^2}}\right)} \qquad (1)$$

where U is the flow velocity, m is the mode order, $\gamma$ is the ratio of specific heats, and empirical constants are k and $\alpha$ [6, 7, 8]. According to Rossiter [7], k = 0.57 and $\alpha$ = 0.25 provide good agreement for this semi-empirical approximation. Figure 9 shows the predicted edge-tone values as well as results from measurements made throughout the entire test at the centerline line and on the test section walls.

A centerline spectrum from the probe at M = 0.8 is shown in Figure 10. At this Mach number, the 16 Hz resonant peak related to the plenum chamber is still very evident. The perforation related edge-tone peak has become more distinct and has increased to 12 kHz, as expected with a higher Mach number.

Interesting responses can be seen from the two transducers installed on the test section diffuser floor at M = 0.8 (Figures 11 and 12). The DIFF1 transducer was located in the vicinity of the camera box. As seen in Figure 11, the camera box triggers severe flow separations with frequencies starting at about 7 kHz. As indicated in Figure 12, the downstream transducer (DIFF2) located on the west side of the centerline, opposite from the camera box, shows no sign of flow disturbances generated by the camera box. This is a fair indication that the diffuser performs quite well; e.g., there is little or no flow separation due to the diffuser geometry.

Figures 13, 14 and 15 show the spectra from the centerline and the diffuser at M = 1.1. From the centerline response (Figure 13) it can be seen that the edge-tone frequency has again increased with Mach number to approximately 15 kHz. In Figures 14 and 15, the spectra for the diffuser transducers show the same effect from the camera box as was seen at M = 0.8.

Figure 16 indicates the centerline spectrum in the porous test section at M = 1.2. The edge-tone spike location has increased to 16 kHz.

### 3.2 Solid Test Section

Fluctuating static pressures in the solid wall test section were measured at Mach 1.4, 1.6, 2.0 and 3.0. Figure 17 shows the dynamic pressure coefficient as a function of Mach number. Frequency spectra at these supersonic Mach numbers are shown in Figures 18 to 21. Compared to centerline spectra at transonic and lower supersonic speeds, the broadband hump at approximately 200 Hz gradually disappears with increasing supersonic Mach number. This suggests that the origin of the broadband noise is the wind tunnel regulating valve.

The resonant spike at 22 Hz, found in all solid test section spectra, corresponds to a natural frequency of the model and model support system. This natural frequency is more pronounced in the solid test section because of increased starting/stopping loads and subsequent vibration associated with high supersonic Mach numbers.

## 4 Conclusions

Static pressure fluctuations were investigated in both porous and solid test sections of the Allied Aerospace North American 7 x 7 foot Trisonic Wind Tunnel. Fluctuating static pressure levels are comparable to most major industrial wind

tunnels at transonic speeds. Dominant freestream acoustic disturbances were found to originate in the plenum chamber and from the perforated test section walls. As expected, the overall noise level in the solid test section at high supersonic Mach numbers is very low.

## References

[1] Mabey, D.G. *Noise Measurements in a Slotted Cryogenic Wind Tunnel*, DRA TR 91062, November 1992.

[2] Igoe, W.B. *Analysis of Fluctuating Static Pressure Measurements in the National Transonic Facility*, NASA Technical Paper 3475, March 1996.

[3] Medved, B.L., Vitic, A, Elfstrom, G.M. *Broadband Noise Measurements in the Transonic Test Section of the VTI T-38 Wind Tunnel*, AIAA-90-1418, June 1990, Seattle, WA.

[4] Julius S. Bendatt and Allan G. Piersol. *Engineering Applications of Correlation and Spectral Analysis*, 1980.

[5] Gotz Paschmann and Patrick W. Daly (Eds.). *Analysis Methods for Multi-Spacecraft Data*, ISSI Scientific Report SR-001 (Electronic Edition 1.1), pp 5-42, 1998.

[6] K.K. Ahuja and J.Mendoza *Effects of Cavity Dimensions, Boundary Layer and Temperature on Cavity Noise with Emphasis on Benchmark Data to Validate Computational Aero-acoustics Codes*, NASA CR 4653, 1995.

[7] Rossiter, J.E. *Wind Tunnel Experiments on the Flow over Rectangular Cavities at Subsonic and Supersonic Speeds*, Ministry of Aviation, Reports and Memoranda No. 3438, October 1966.

[8] Komerath, N.M., Ahuja, K.K., and Chambers, F.W. *Prediction and Measurement Flows Over Cavities*, AIAA 25th Aerospace Sciences Meeting, January 11-15, AIAA 82-022, 1987.

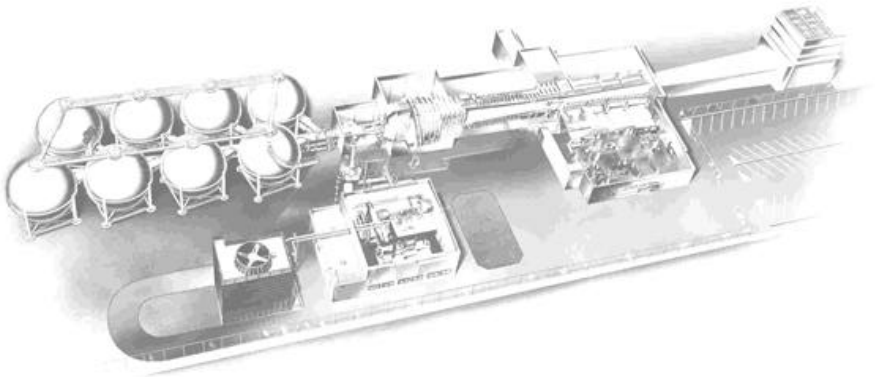

Fig. 1. Allied Aerospace 7 x 7 foot Trisonic Wind Tunnel

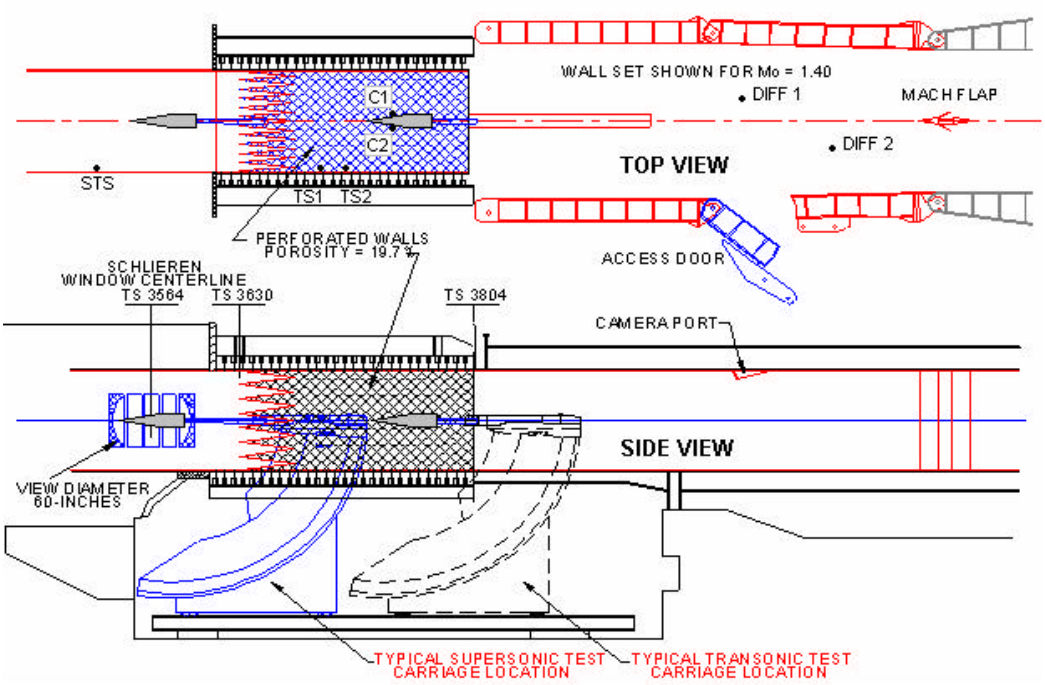


Fig. 2. Tandem Test Section Configuration and Transducer Locations

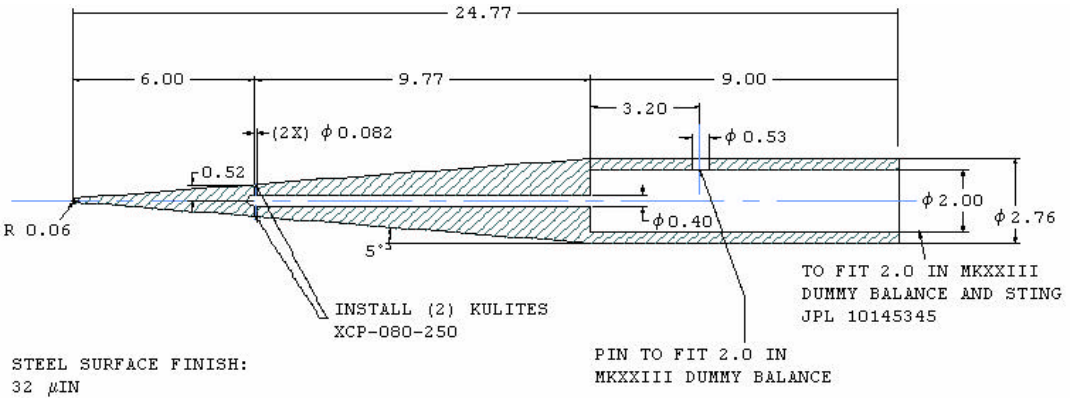


Fig. 3. Ten-Degree Cone Probe

Fig. 4. Ten-Degree Cone Probe Installed in the Solid Test Section

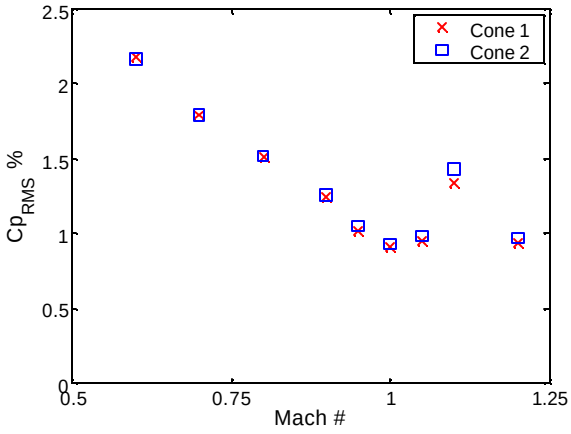


Fig. 5. Centerline Cone Probe Measurements in the Porous Test Section

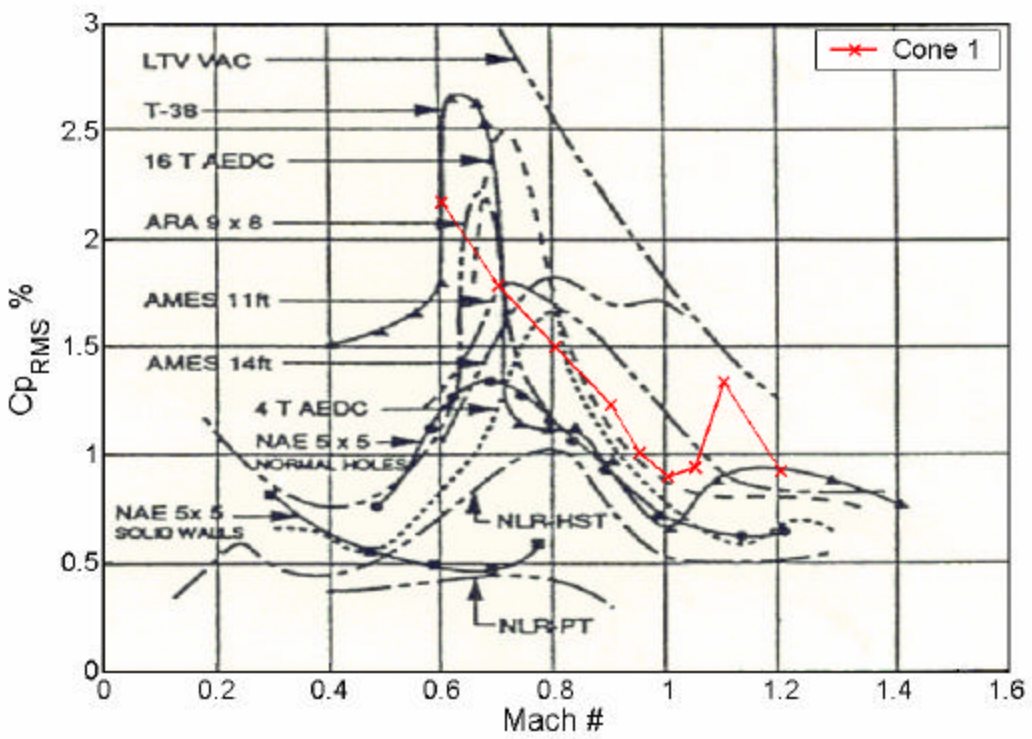


Fig. 6. Transonic Wind Tunnels Noise Level Comparison

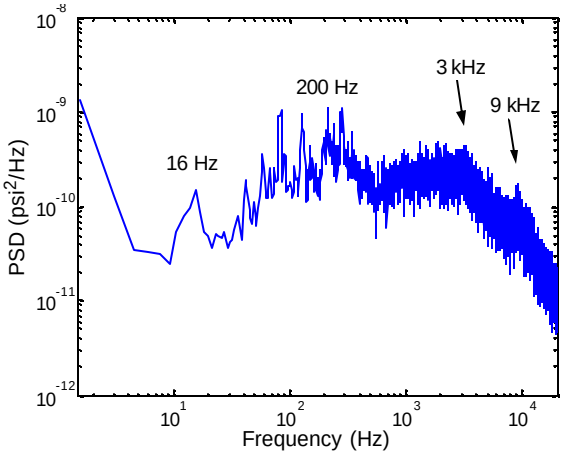


Fig. 7 Centerline, M = 0.6

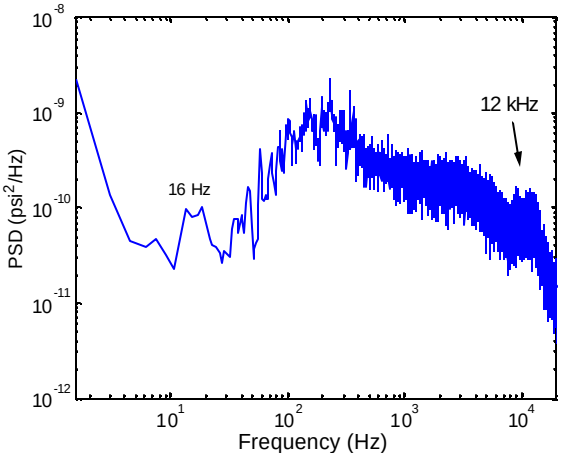


Fig. 10 Centerline, M = 0.8

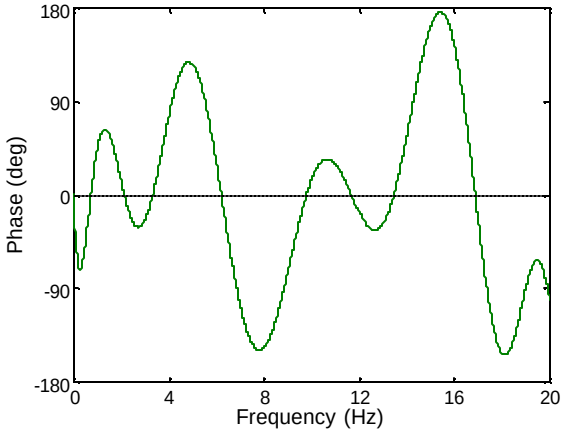


Fig. 8 Phase between Two Adjacent Transducers on the Perforated TS Wall, M = 0.6

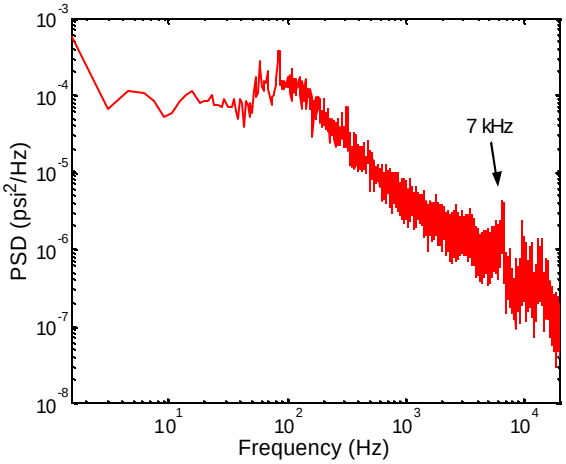


Fig. 11 Diffuser 1, M = 0.8

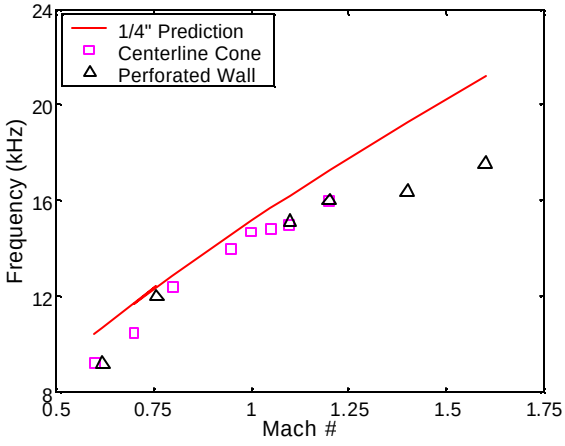


Fig. 9 Edge-Tone Frequencies vs. Mach # (Prediction from Rossiter, Eq.1)

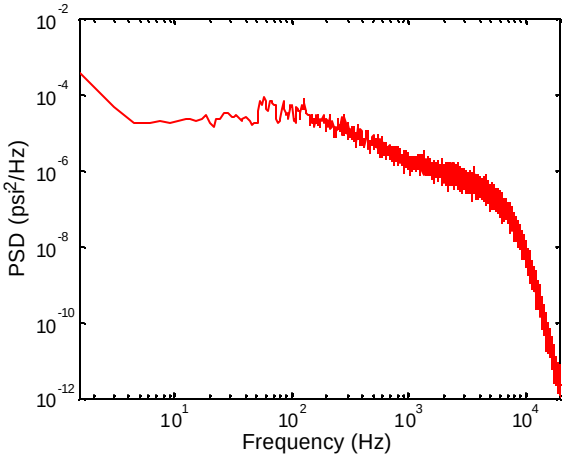


Fig. 12 Diffuser 2, M = 0.8

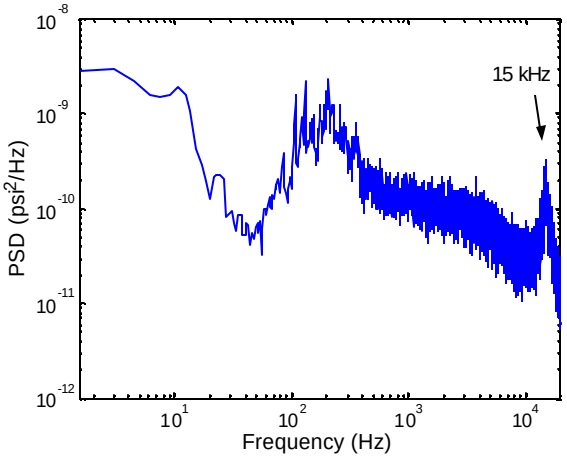


Fig. 13 Centerline, M =1.1

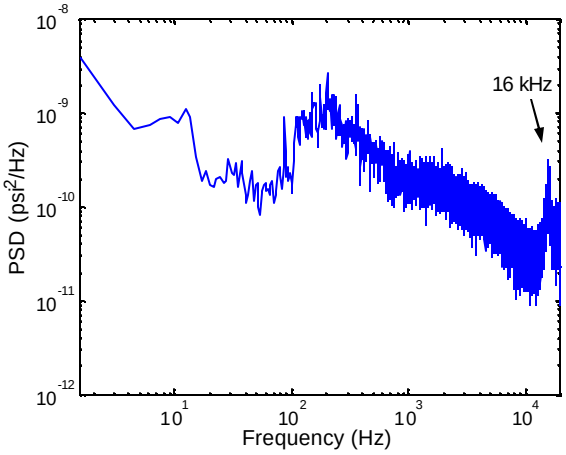


Fig. 16 Centerline, M = 1.2

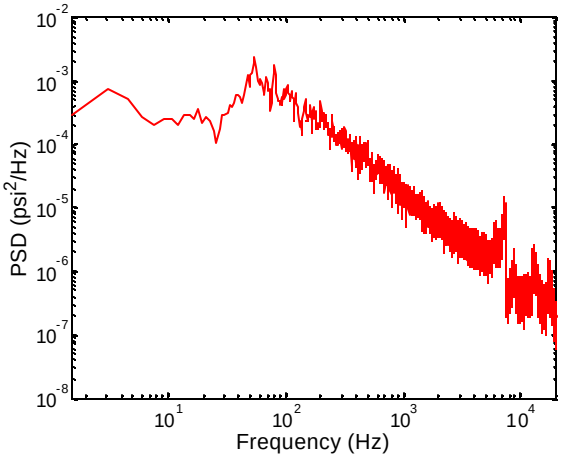


Fig. 14 Diffuser 1, M = 1.1

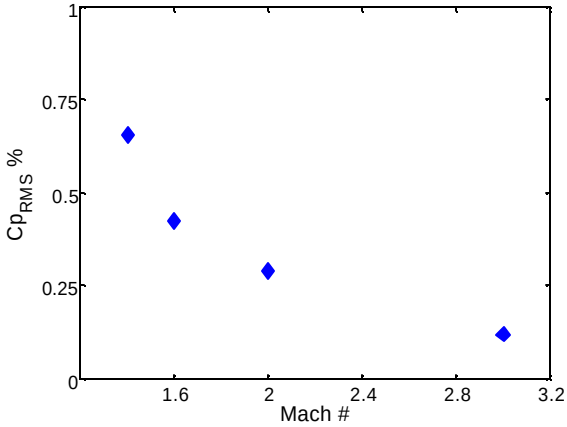


Fig. 17 Dynamic Pressure Coefficients in the Solid Test Section

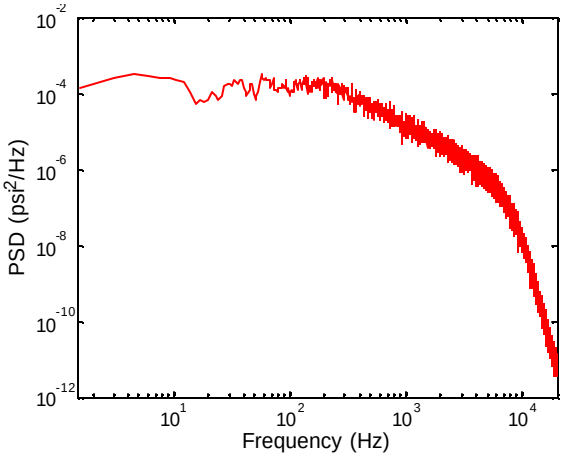


Fig. 15 Diffuser 2, M = 1.1

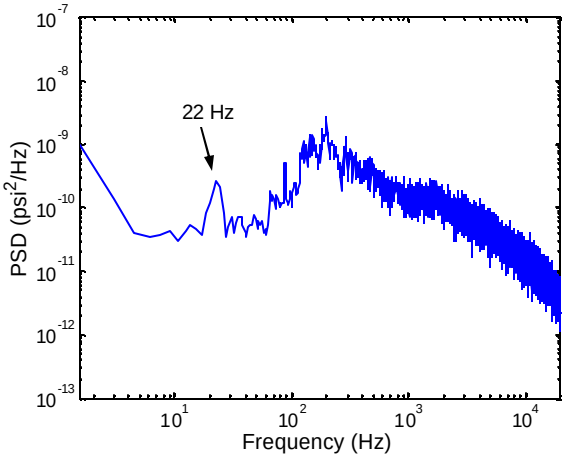


Fig. 18 Centerline, M = 1.4, Solid TS

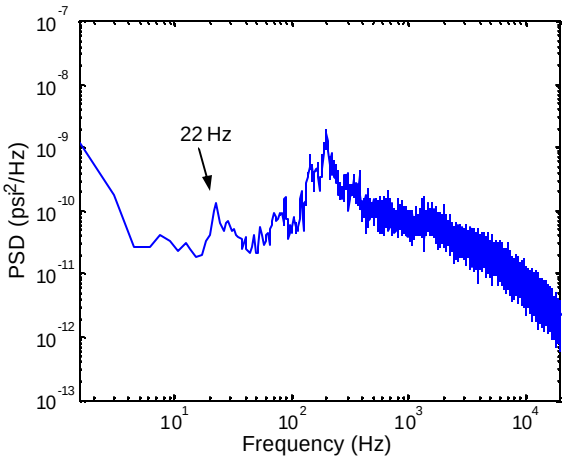


Fig. 19 Centerline, M = 1.6, Solid TS

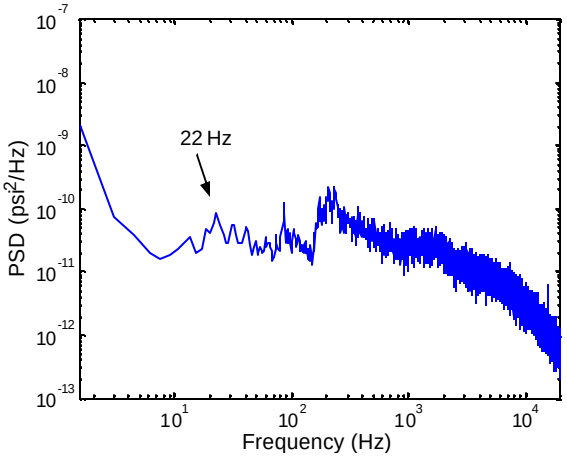


Fig. 20 Centerline, M = 2, Solid TS

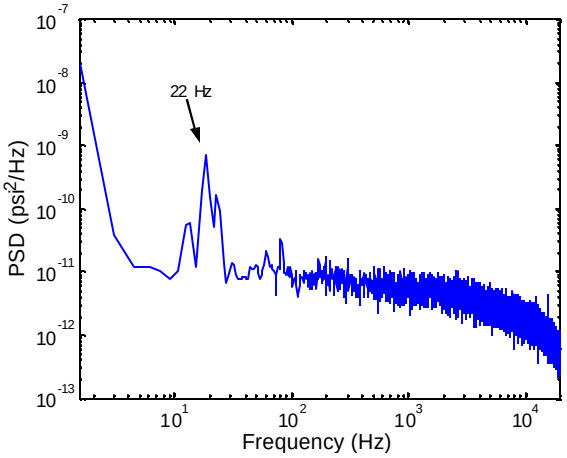


Fig. 21 Centerline, M = 3, Solid TS